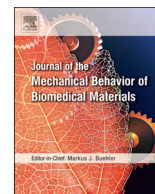




Contents lists available at ScienceDirect

Journal of the Mechanical Behavior of Biomedical Materials

journal homepage: www.elsevier.com/locate/jmbbm

Surface functionalization of polylactic acid fibers with alendronate groups does not improve the mechanical properties of fiber-reinforced calcium phosphate cements

Daniela-Geta Petre^a, Nathan W. Kucko^{a,b}, Anna Abbadessa^{c,d}, Tina Vermonden^c, Alessandro Polini^a, Sander C.G. Leeuwenburgh^{a,*}

^a Department of Regenerative Biomaterials, Radboud University Medical Center, Philips van Leydenlaan 25, Nijmegen 6525 EX, the Netherlands

^b CAM Bioceramics B. V., Zernikedreef 6, Leiden 2333 CL, the Netherlands

^c Department of Pharmaceutics, Utrecht Institute for Pharmaceutical Sciences (UIPS), Faculty of Science, Utrecht University, Utrecht 3508 TB, the Netherlands

^d Department of Fibre and Polymer Technology, School of Engineering Sciences in Chemistry, Biotechnology and Health, Royal Institute of Technology, KTH, Teknikringen 56-58, 10044 Stockholm, Sweden

ARTICLE INFO

Keywords:

Calcium phosphate cements
Reinforcement
Polyester
Affinity
Alendronate

ABSTRACT

Calcium phosphate cements (CPCs) are frequently used as synthetic bone substitute, but their intrinsic low fracture toughness impedes their application in highly loaded skeletal sites. However, fibers can be used to reduce the brittleness of these CPCs provided that the affinity between the fibers and cement matrix facilitates the transfer of loads from the matrix to the fibers. The aim of the present work was to improve the interface between hydrophobic polylactic acid (PLA) microfibers and hydrophilic CPC. To this end, calcium-binding alendronate groups were conjugated onto the surface of PLA microfibers via different strategies to immobilize a tunable amount of alendronate onto the fiber surface. CPCs reinforced with PLA fibers revealed toughness values which were up to 50-fold higher than unreinforced CPCs. Nevertheless, surface functionalization of PLA microfibers with alendronate groups did not improve the mechanical properties of fiber-reinforced CPCs.

1. Introduction

Since their discovery in the early 1980s, calcium phosphate cements (CPCs) have been increasingly used as synthetic bone substitutes due to their chemical similarity with the mineral phase of bone. Despite their excellent osteocompatibility and handling properties (Kruger and Groll, 2012), widespread usage of CPCs is limited by their intrinsic low fracture toughness, which impedes their application in highly loaded skeletal sites (Larsson and Hannink, 2011).

Various strategies have been adopted to reduce the intrinsic brittleness of CPCs. So far, reinforcement of CPCs with fibers has been the most successful approach to toughen CPCs. To render CPCs resorbable, a biodegradable fiber should be selected to provide mechanical reinforcement to the cement matrix, followed by subsequent degradation of the fibers and concomitant ingrowth of newly formed bone into the pores (Gunnella et al., 2017; Maenz et al., 2017). Aliphatic polyester fibers have been used most extensively for reinforcement of CPCs due to their tunable degradation rate and low toxicity of their degradation by-products. Several studies on fiber reinforcement of CPCs have varied

the composition of these polyester fibers by using either polylactic acid (PLA), poly-ε-caprolactone (PCL) or poly(lactic-co-glycolic acid) (PLGA) copolymers (Xu and Quinn, 2002; Zuo et al., 2010). In addition, the influence of fiber length (Maenz et al., 2014) and amount (Castro et al., 2017) of these polyester fibers on the fiber reinforcement efficacy has been investigated. Nevertheless, only few studies (Canal et al., 2014; Maenz et al., 2016) focused on the adhesion between polyester fibers and the inorganic matrix of CPCs, although it is well recognized that the efficacy of fiber reinforcement strongly depends on the adhesion between fibers and inorganic matrices. Specifically, polyester fibers such as PLA are hydrophobic whereas CPCs are hydrophilic. This mismatch in chemical properties might compromise the binding affinity between polyester fibers and the CPC matrix, thereby reducing the fiber reinforcement efficacy.

As mentioned above, fiber reinforcement can only be effective when the affinity between both composite components is optimized since loads are essentially transferred from the matrix to the reinforcing fibers at their interface. An excessively strong bond between the two components will lead to fiber rupture without sufficient energy

* Correspondence to: Department of Regenerative Biomaterials, Radboud University Medical Center, PO Box 9101, 6500 HB Nijmegen, the Netherlands
E-mail addresses: daniela-geta.petre@radboudumc.nl (D.-G. Petre), sander.leeuwenburgh@radboudumc.nl (S.C.G. Leeuwenburgh).

<https://doi.org/10.1016/j.jmbbm.2018.11.003>

Received 15 July 2018; Received in revised form 1 November 2018; Accepted 2 November 2018

Available online 03 November 2018

1751-6161/ © 2018 Elsevier Ltd. All rights reserved.

dissipation, whereas an excessively weak interface leads to fiber pull-out and poor energy dissipation (Kruger and Groll, 2012). Consequently, it is of utmost importance to tune the affinity between fibers and their surrounding matrix. In that respect, fibers of tunable calcium-binding affinity would allow for a systematic investigation and optimization of the efficacy of fiber reinforcement of calcium-containing CPCs.

Previously, we successfully conjugated the amino-bisphosphonate alendronate onto the surface of hydrophobic PLLA sub-micron fibers (Polini et al., 2017). This functionalization strategy was selected in view of the strong capacity of alendronate to bind to calcium ions in hydroxyapatite crystals (Pascaud et al., 2014). We used PLLA sub-micron fiber mats obtained by means of electrospinning and subjected them to an aminolysis procedure in order to obtain discrete fibers of tunable aspect ratio. Following this aminolysis procedure, alendronate was conjugated onto the fiber surface via glutaraldehyde-mediated chemistry. Our results demonstrated improved affinity of the alendronate-functionalized fibers to calcium-containing CPCs. However, incorporation of these alendronate-modified sub-micron fibers in the cement matrix did not have any stimulatory effect on the reinforcement of CPCs since these discrete nanofibers were essentially too small for effective reinforcement of the nanoporous CPC; the dimensions of the fibers were comparable with the size of the nanopores in the tested cement matrix (data not shown).

Consequently, the main aim of the present study was to investigate the effect of alendronate-functionalized microfibers instead of sub-micron fibers on the mechanical properties of CPCs. We hypothesized that this functionalization strategy would i) improve the affinity of the hydrophobic PLA microfibers to the hydrophilic cement and ii) enhance the reinforcing efficacy of these fibers upon incorporation into CPC. To this end, we covalently functionalized alendronate onto micron-scale PLA fibers by means of three different types of strategies based on fragmentation of long PLA fibers using either chemical or manual cutting. Chemical cutting involved fiber fragmentation by means of aminolysis of PLA fibers which was followed by conjugation of alendronate via either i) aldehyde chemistry or ii) a Michael addition reaction with acrylated alendronate (AcrALE). The latter functionalization strategy was designed to improve the specificity of the reaction, thereby enhancing the control over the reaction and the chemical stability of the conjugation. The third conjugation strategy involved polydopamine-assisted immobilization of alendronate onto manually cut PLA fibers. This method was adopted to decouple fiber cutting from alendronate conjugation through an aminolysis-independent and universally applicable functionalization strategy.

The surface morphology, amine and alendronate content of the functionalized fibers were analyzed using electron microscopy, several biochemical assays, and inductively coupled plasma-optical emission spectroscopy (ICP-OES), respectively. Subsequently, the functionalized fibers were incorporated into CPCs followed by evaluation of the mechanical properties of the fiber-reinforced composites to determine the flexural strength, stiffness and work of fracture (WOF) as a measure of composite toughness.

2. Materials and methods

Commercially available polylactic acid (PLA) microfibers Type 260 (6 mm length, 11 μ m diameter), tensile strength between 210 and 558 MPa, tensile modulus between 3 and 6 GPa were kindly supplied by Trevira (Bobingen, Germany). We selected these PLA microfibers in view of their higher tensile strength as compared to unreinforced CPC typically (\sim 1–10 MPa) (Bohner, 2001). Moreover, PLA is widely used in numerous biomedical devices. The biodegradation rate of PLA-based devices is rather slow (months to years) which allows for sustained reinforcement of CPCs. Finally, PLA microfibers were selected since previous studies revealed that PLA fibers can be cut chemically via aminolysis (Kim and Park, 2008; Polini et al., 2017) to control their

aspect ratio and allow further chemical functionalization. α -tricalcium phosphate (α -TCP) microparticles were provided by CAM Bioceramics (Leiden, The Netherlands). Alendronic acid (purity 95%) was purchased from AK Scientific (Union City, CA). Tris(hydroxymethyl)aminomethane (Tris buffer) was obtained from Thermo Fischer Scientific (Waltham, MA), while all the other chemicals were obtained from Sigma Aldrich (St Louis, MO).

2.1. Fragmentation and chemical functionalization of PLA microfibers

2.1.1. Fiber fragmentation by means of aminolysis of PLA fibers

PLA fibers were subjected to aminolysis and subsequent transverse fragmentation to reduce their length, as previously reported (Kim and Park, 2008). Briefly, fibers were aminolyzed at a fiber content of 2.5 mg/ml for time periods between 6 h and 15 h in solutions of ethylenediamine (EDA) in isopropanol (IPA) (3% w/v or 5% w/v) at 37 °C. The fibers were fragmented every 2 h during the aminolysis procedure by sonication, each time for 1 min (UP100H, Hielscher Ultrasonics, Teltow, Germany) at a 100% amplitude and a 100% duty cycle. Subsequently, the supernatant was discarded and the fibers were washed three times with Milli-Q. Finally, the aminolyzed fibers were freeze-dried and chemically functionalized with either pure alendronate (using glutaraldehyde chemistry) or acrylated alendronate (using a Michael addition reaction) as explained below.

2.1.2. Functionalization of aminolyzed PLA fibers with alendronate using aldehyde chemistry

Alendronate (ALE) molecules were conjugated to the surface of the aminolyzed PLA fibers using glutaraldehyde chemistry (Uquillas Paredes et al., 2014) by incubating fibers (2.5 mg/ml) in a 15 mM alendronic acid aqueous solution supplemented with a 5% v/v glutaraldehyde solution which was mixed on a rotating wheel at 40 rpm, at room temperature overnight. Fibers were washed three times with Milli-Q for 10 min, incubated in a 15 mM glycine aqueous solution to block any residual aldehyde groups derived from glutaraldehyde, and finally washed twice with Milli-Q before freeze drying. As a control experiment, pristine fibers (without aminolysis treatment) were also incubated in a 15 mM alendronic acid solution and washed three times with Milli-Q. The aminolyzed PLA fibers functionalized with ALE are denoted as PLA-ALE.

2.1.3. Functionalization of aminolyzed PLA fibers with alendronate using a Michael reaction

Since the imine bond formed through glutaraldehyde chemistry is hydrolytically labile, we also synthesized acrylated alendronate (AcrALE) to allow for a Michael addition reaction with amine groups present on the surface of aminolyzed PLA fibers, thereby offering more control and a higher selectivity of the reaction and avoiding potential self-crosslinking of fibers. To this end, alendronic acid (1 g, 4 mmol) was dissolved in 40 ml of 2 wt% NaOH solution and kept at 0 °C by external ice-bath cooling. Acryloyl chloride (1.2 ml, 16 mmol) was added in four portions over 1 h period and the pH was adjusted back to 10 after adding the 3rd and 4th portion of the monomer. The mixture was stirred for 1.5 h at room temperature followed by extraction with ethyl acetate two times (Varghese et al., 2009). The aqueous phase was freeze-dried and the obtained powder was washed with cold methanol. The precipitate was collected by centrifugation and dried under vacuum to obtain the acrylamidoalkyl bisphosphonate (AcrALE) (627 mg, 63%) as a white solid. Subsequently, the aminolyzed fibers, obtained as described above, were conjugated with AcrALE via a Michael addition reaction by incubating them at 2 mg/ml in 0.1 M HEPES buffer containing AcrALE at a 1:2 molar ratio between amine and AcrALE groups.

2.1.4. Functionalization of manually cut PLA fibers with alendronate using polydopamine-assisted immobilization

PLA fibers were cut manually by means of a scalpel in two different

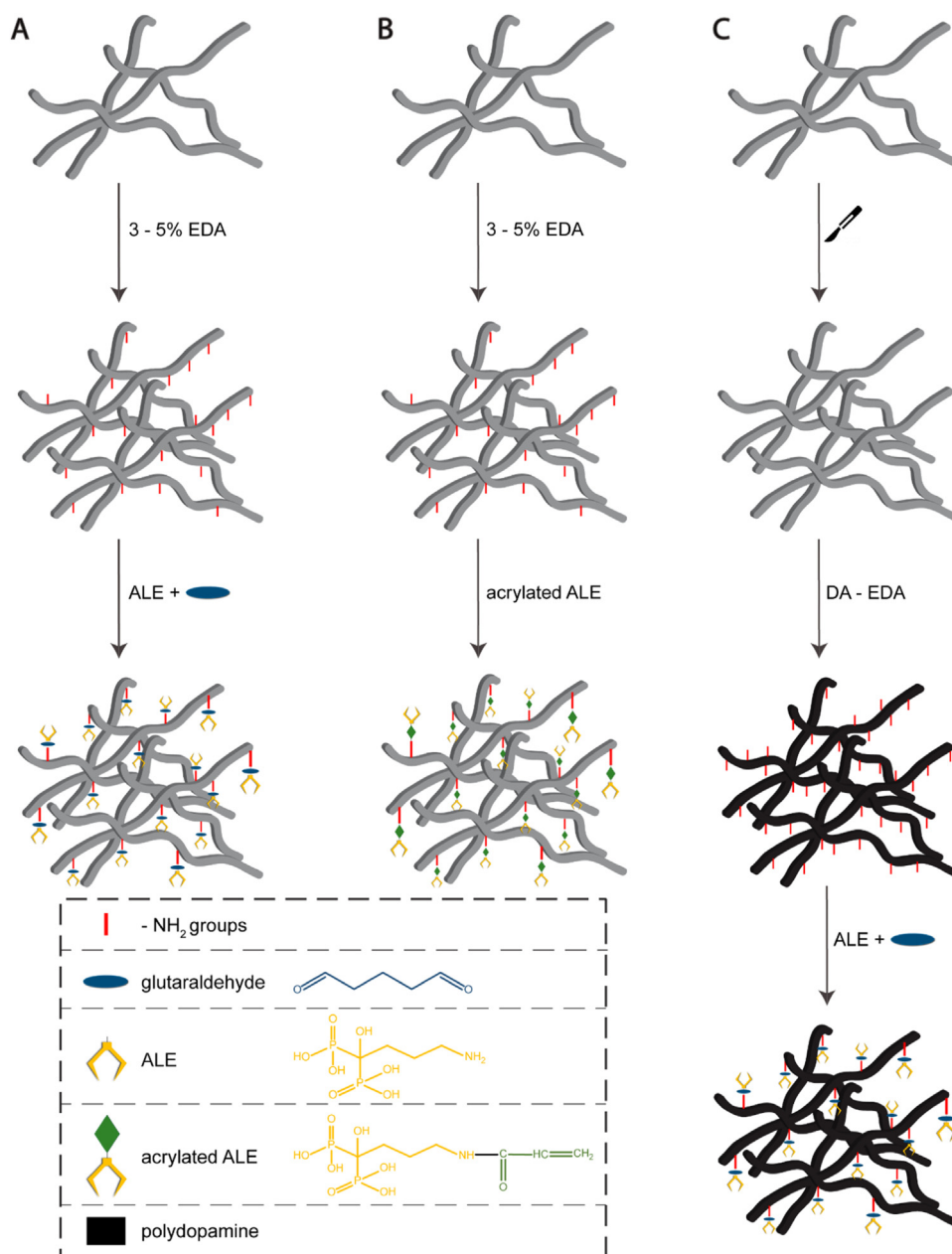


Fig. 1. A) Functionalization of aminolyzed PLA fibers with alendronate using aldehyde chemistry or B) Michael reaction, C) Functionalization of manually cut PLA fibers with alendronate using polydopamine-assisted immobilization.

fiber lengths: 1.5 mm and 3 mm. These manually cut fibers were immersed at room temperature in an aqueous solution containing different amounts of dopamine (DA) hydrochloride (1–10 mg/ml) and EDA (0.05% w/v) in 10 mM Tris buffer (pH 8.5) for 12 h under gentle agitation. These conditions were selected based on previous optimization of the type of amine (ethylenediamine or hexamethylenediamine), the amine concentration (between 0.05% and 0.2% w/v) and the polydopamine immobilization time (12 h, 24 h or 48 h). Subsequently, the fibers were washed three times with Tris buffer and Milli-Q to remove loosely bound polydopamine followed by freeze-drying. Using this PDA-EDA functionalization method, a high density of amine groups were immobilized at the fiber surface. Finally, these generated amine groups were used to conjugate ALE onto the PDA-EDA coated fibers using glutaraldehyde chemistry as described above.

The PLA fibers coated with PDA are denoted as PLA-PDA, while the fibers functionalized with ALE via PDA immobilization are denoted as PLA-PDA-ALE. Fig. 1 summarizes the fiber fragmentation methods and

functionalization strategies adopted herein.

2.2. Physico-chemical characterization of alendronate-functionalized microfibers

The density of amine groups at the surface of PLA fibers was determined by means of the 2,4,6-trinitrobenzenesulfonic acid (TNBS) assay for aminolyzed fibers and the Acid Orange II (AO II) assay for PDA-EDA coated fibers according to methods described elsewhere (Li et al., 2011; Wang et al., 2012). Additionally, fluorescamine was reacted to the fiber surface to visualize the presence of amine groups by incubating 1 mg of fibers into a solution of 0.5 mg/ml fluorescamine in acetone for 1 h, after which the fibers were washed twice with Milli-Q. Images were collected using bright-field and fluorescence microscopy using a fluorescence microscope Axio Imager Z1 Microscope (Carl Zeiss Micro Imaging GmbH, Göttingen, Germany) equipped with a digital camera (AxioCam MRc5, Carl Zeiss AG Light Microscopy). The fiber

length was assessed using the bright-field micrographs from at least 100 randomly selected fibers using ImageJ software (Wayne Rasband, Research Services Branch, National Institute of Mental Health, Bethesda, MD). The chemical structure of AcrALE was confirmed by ^1H nuclear magnetic resonance (NMR) using deuterium oxide (D_2O) as solvent. Inductively coupled plasma-optical emission spectroscopy (ICP-OES; iCAP 6000, Thermo Fisher Scientific) analysis was carried out to determine the phosphorous content of the fibers as a means to quantify the amount of conjugated alendronate. This analysis was performed in triplicates for all alendronate-functionalized fibers after digesting the fibers overnight in a 5% nitric acid solution. Further qualitative analysis was carried out by means of Fourier transform infrared spectroscopy (FTIR) using a spectrum two system (Perkin Elmer, Groningen, The Netherlands) at a step size of 4 cm^{-1} and 4 scans/sample in order to investigate the surface chemistry of PLA fibers functionalized with ALE via PDA immobilization.

2.3. Fiber affinity for hydroxyapatite

The affinity of functionalized PLA fibers for hydroxyapatite (HA) surfaces was investigated by soaking alendronate-functionalized fibers onto calcium phosphate (CaP) ceramics. HA disks were prepared by pressing HA powder (Merck Darmstadt, Germany) into disks in hardened steel-pressing dies (diameter: 1 cm) at 7 MPa (rough samples) for 1 min followed by sintering for 4 h at $1300\text{ }^\circ\text{C}$, with heating and cooling rates of $2\text{ }^\circ\text{C}/\text{min}$ (Polini et al., 2014). Specimens were then immersed in phosphate-buffered saline (PBS) solution for 1 day at room temperature to allow for phase transformation toward the apatite phase and finally stored in dry conditions until further use. For the affinity studies, HA samples were incubated in an aqueous suspension of fibers (2.5 mg/ml) for 4 h under gentle mixing, washed three times for 10 min with Milli-Q, dried, Au-sputtered and imaged by means of scanning electron microscopy (SEM, JEOL 6310, Jeol Corp., Tokyo, Japan). During incubation, the disks were placed vertically to avoid sedimentation of fibers on CaP surfaces.

2.4. Preparation of fiber-reinforced calcium phosphate cements

Fiber-reinforced calcium phosphate cements were prepared by manual mixing of the solid powder phase (α -TCP) to which PLA fibers were previously added, with the liquid phase (4% w/v Na_2HPO_4). A liquid/powder (L/P) ratio of 0.5 was applied. Weight fractions of the fibers in the cement were fixed at either 2.5 wt% or 5 wt%. Fiber length was varied between 1.2 mm and 3 mm for the chemically cut fibers or between 1.5 mm and 3 mm for the manually cut fibers. After manual mixing of the three components, the fiber-reinforced pastes were transferred to $4 \times 4 \times 25\text{ mm}^3$ silicone molds and stored at room temperature for 12 h. Subsequently, the hardened composite samples were incubated in PBS for 3 days at $37\text{ }^\circ\text{C}$ to allow for conversion of α -TCP to HA.

2.5. Mechanical properties of the fiber-reinforced CPCs

A standard three-point flexural test with a span of 20 mm was performed on rectangular $4 \times 4 \times 25\text{ mm}^3$ specimens at a crosshead speed of 1 mm/min. The composite materials reinforced with amino-lyzed fibers were tested on a universal testing machine (MTS Systems, 858 mini bionix II), whereas the composites reinforced with functionalized fibers obtained via PDA-assisted immobilization were tested on a different testing bench (LS5, Lloyd Instruments/Ametek). From the three-point flexural test, the flexural strength, flexural modulus of elasticity, and work of fracture (WOF, as a measure of toughness) were calculated from the load-displacement curves as follows:

$$\text{Flexural strength: } S_c = \frac{3P_{\max} L}{2bh^2},$$

where P_{\max} is the maximum load on the load–displacement curve, L is the flexure span, b is the specimen width and h is the specimen thickness.

$$\text{Flexural modulus: } E_{\text{bend}} = \frac{mL^3}{4bh^3},$$

where m is the slope of tangent to the initial straight-line portion of the load–displacement curve.

$$\text{Work of fracture: } \text{WOF} = \frac{A}{bh},$$

where A is the area under the load–displacement curve.

For all the composite specimens, the test was stopped at a maximum crosshead displacement of 4 mm and the WOF values were calculated by integrating the area under the stress-strain curve. Fourteen specimens were tested for each group ($n = 14$) and outliers were eliminated by using the interquartile range rule.

2.6. X-ray diffraction

After mechanical testing, solid samples were grinded to powder and X-ray diffraction was applied to determine the crystal phases of the cement composites. The phase composition of pure CPC and CPCs reinforced with PLA fibers at various weight fractions or modified using different functionalization strategies were analyzed using an X-ray diffraction system (XRD Panalytical, Philips, The Netherlands) operated at 45 kV and 30 mA.

2.7. Morphological assessment and nano-CT analysis

Morphological assessment of the fibers and the fractured composite samples was performed using SEM. Samples were coated with a 10 nm chromium layer and images were acquired at 5 kV.

To visualize the fiber distribution and porous structure of the CPCs, the composite samples were scanned vertically along the X-ray beam by using a nano-CT imaging system (NanoTom Phoenix, General Electric, Wunstorf, Germany). Samples were recorded using a voxel size of 2.36 μm , an X-ray source of 90 kV/110 μA , an exposure time of 500 ms without the application of a filter. The obtained projected files were reconstructed using dedicated software (General Electric, Germany) and analyzed with CT-Analyser software (version 1.17.7.2+; Bruker, Kontich, Belgium). The volume of interest (VOI) was defined manually by selecting an area of $3.4 \times 4.12\text{ mm}^2$ and a total of 1500 slices (i.e. approx. 3.55 mm in height). In order to quantify the fiber volume in the specimens, a simple thresholding method was applied, with a single threshold value chosen to separate the porous space and fibers from the cement phase in the composite. The values represent the average of three individual samples and were normalized to the control sample (sample without any fibers). CTvox software (version 3.0.0 r1114, Bruker, Kontich, Belgium) was applied for 3D visualization.

2.8. Statistics

All data were expressed as mean \pm standard deviation. Statistical analysis of all chemical assays was performed by one-way analysis of variance (ANOVA) followed by a Bonferroni post hoc test. The mechanical properties were analyzed statistically by means of two-way ANOVA followed by a Tukey post hoc test. For all tests, the level of significance was set at $p < 0.05$. All statistical tests were performed using GraphPad Prism software (GraphPad Software, Inc., La Jolla, CA).

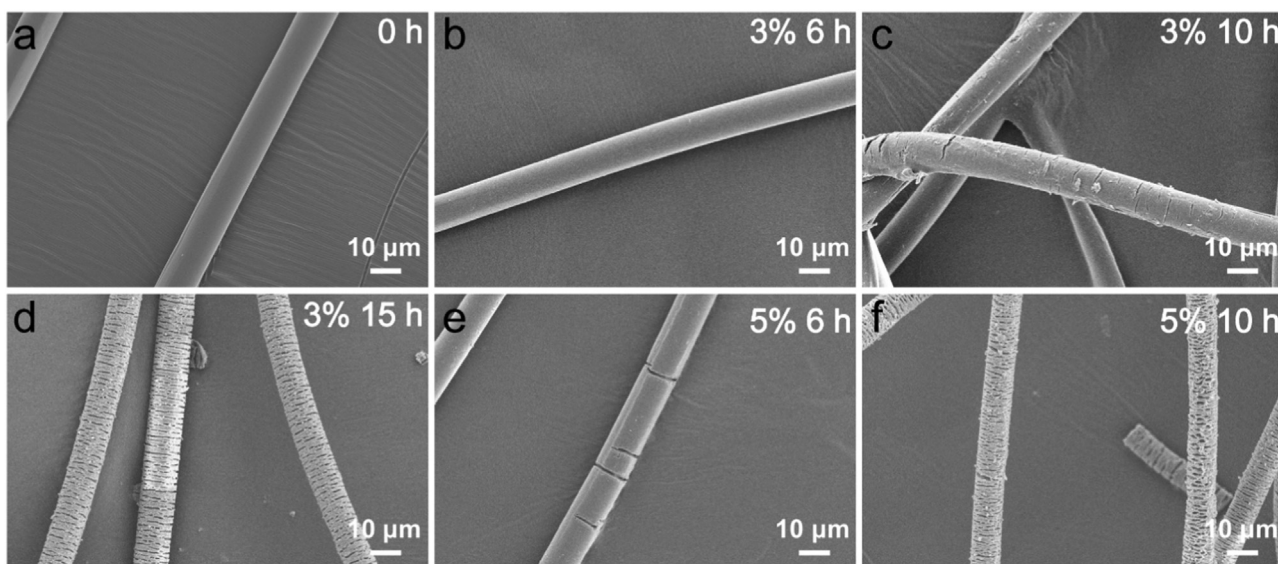


Fig. 2. SEM images of PLA fibers aminolyzed for various time periods at different amine (EDA) concentrations: (a) pristine PLA fibers, (b–d) 3% EDA for 6 h, 10 h and 15 h of aminolysis, (e–f) 5% EDA for 6 h and 10 h of aminolysis.

3. Results

3.1. Functionalization of aminolyzed PLA fibers with alendronate using aldehyde chemistry or Michael reaction

To tune the length of discrete PLA microfibers and introduce amine groups at their surface, PLA fibers were aminolyzed for different time periods at different aminolysis concentrations.

Fig. 2(a) presents the smooth surface of PLA control fibers, whereas aminolyzed PLA fibers displayed a patterned roughness that increased with increasing aminolysis time. As shown in Fig. 2(b–d), cracks appeared at the surface of PLA fibers aminolyzed for 10 h in a 3% EDA solution. PLA fibers aminolyzed in solutions containing 5% EDA revealed a severely eroded surface morphology characterized by clear transversal cracks along the surface of the fibers, which suggests that these aminolysis conditions were too harsh for this type of polyester.

Fig. 3 shows the effect of aminolysis concentration and time on fiber length in a quantitative manner. For a 3% EDA concentration (Fig. 3(a)), the shortest aminolysis time (6 h) was sufficient to induce fragmentation of the fibers to an average length of 3000 μm (aspect ratio 270), while the highest aminolysis time (15 h) yielded fibers that were 1000 μm long (aspect ratio 115). For an increased aminolysis concentration of 5% EDA, the mean fiber length decreased below 1000 μm down to values ranging from 650 μm to 350 μm . As shown in Fig. S1(a), the amine content of the aminolyzed PLA fibers increased with increasing aminolysis time.

Maximum and minimum amine contents were observed after aminolysis times of 12 h (~ 600 nmol/mg of fiber) and 6 h (~ 100 nmol/mg of fiber) for the 5% EDA concentration, whereas amine groups were not detected on PLA control fibers. To visualize these amine groups at the fiber surface, fluorescamine was conjugated to the amine groups and visualized using fluorescence microscopy. Fig. S1(b) shows that the fibers were homogeneously covered with amine groups after aminolysis, which proves the efficiency of this process to introduce active moieties for subsequent chemical functionalization.

In order to increase the affinity of PLA fibers to CaP, we conjugated alendronate as a Ca^{2+} -binding moiety to the surface of aminolyzed PLA fibers by means of either glutaraldehyde or Michael addition chemistry. For the latter, acrylated alendronate was synthesized and its chemical structure was proven by H NMR. The presence of the signals at 5.8 and 6.2 ppm, representative of the two vinyl protons of the acrylate group, confirm the functionalization of the amine groups of alendronate with acrylate groups (Fig. S2).

Fig. 4 presents the amount of alendronate functionalized on the surface of aminolyzed PLA fibers by means of either glutaraldehyde or Michael addition chemistry. For both conjugation methods, the amount of alendronate increased with increasing aminolysis time, leading to a maximum of alendronate amount of ~ 6.5 μg ALE/mg of fiber for the highest amine group density (corresponding to 15 h aminolysis time). Furthermore, the alendronate amount increased with increasing aminolysis concentrations (3% EDA vs. 5% EDA) for glutaraldehyde-mediated conjugation. These results confirm that the aldehyde-

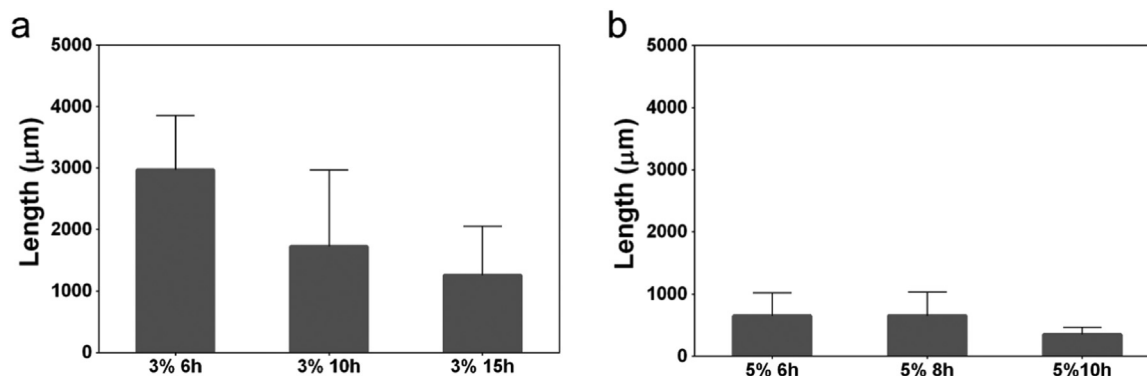


Fig. 3. Fiber length as a function of aminolysis time at a concentration of (a) 3% EDA and (b) 5% EDA.

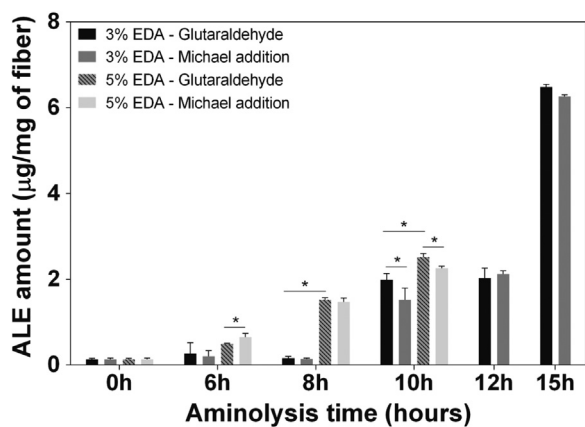


Fig. 4. Quantification of alendronate amount conjugated to aminolyzed PLA fibers using either glutaraldehyde or Michael addition chemistry by means of ICP-OES; lines above the bars indicate statistically significant differences among groups (* $p < 0.05$).

mediated coupling reaction is directly correlated with the amount of free amine groups on the fiber surface as detected using the TNBS assay.

However, the differences regarding the amount of alendronate conjugation using either glutaraldehyde or Michael addition chemistry were small. Therefore, we used glutaraldehyde chemistry for further experiments since no additional advantage was found for the more time-consuming Michael addition method. Moreover, in view of the undesired effects of excessive surface erosion on the functional properties of fibers (Causa et al., 2010), we selected a relatively mild aminolysis concentration of 3% EDA concentration and aminolysis times of 6 h, 10 h and 15 h (corresponding to 3 mm, 1.7 mm and 1.2 mm fiber lengths) for further studies.

3.2. Functionalization of manually cut PLA fibers with alendronate using polydopamine-assisted immobilization

As shown in Fig. 5, the surface of the PLA fiber was smooth, while PLA-PDA samples were homogeneously covered with a dense and rough dopamine coating. FTIR analysis (Fig. S3) confirmed that the newly formed layer on the surface of pristine PLA fibers for PLA-PDA and PLA-PDA-EDA samples correspond to the immobilization of polydopamine, as indicated by two distinct absorption peaks at 1625–1597 cm^{-1} (C=C

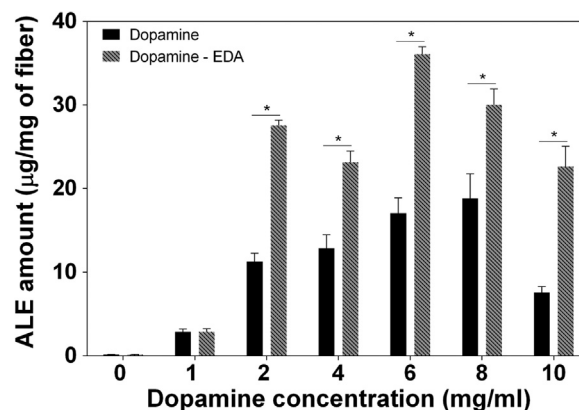


Fig. 6. Quantification of alendronate amount conjugated to polydopamine-coated PLA fibers prepared in the presence or absence of EDA; lines above the bars indicate statistically significant differences among groups (* $p < 0.05$).

resonance vibrations in the aromatic ring) and 1507–1515 cm^{-1} (N–H shearing vibrations). The small redshift of these peaks towards lower wavenumbers corresponds to the formation of intermolecular interactions between DA and EDA (Yang et al., 2015).

Fig. S4(a) presents the quantification of the amount of amine groups at the surface of PLA fibers coated with either a PDA or an amine-enriched PDA-EDA layer. Compared to pristine PLA fibers, the amine content increased for all dopamine concentrations with or without the addition of EDA. However, by increasing the concentration of dopamine above 6 mg/ml, the amine content decreased for both groups. Fig. S4(b) shows the amount of conjugated alendronate as a function of dopamine coating time. For a dopamine concentration of 6 mg/ml, the conjugation efficiency decreased with increasing the dopamine coating time from 12 h to 48 h.

Fig. 6 shows the amount of alendronate conjugated onto PLA-PDA coated fibers using glutaraldehyde chemistry. The amount of alendronate conjugation strongly depended on both the dopamine concentration and the incorporation of additional EDA groups. For PLA fibers covered with a PDA layer using 6 mg/ml dopamine, the amount of alendronate conjugation was equal to $\sim 18 \mu\text{g ALE/mg}$ of fiber. This amount was doubled to $\sim 35 \mu\text{g ALE/mg}$ of fiber for the same dopamine concentration by adding EDA. However, when increasing the dopamine concentration above 6 mg/ml, a linear decrease in the amount of

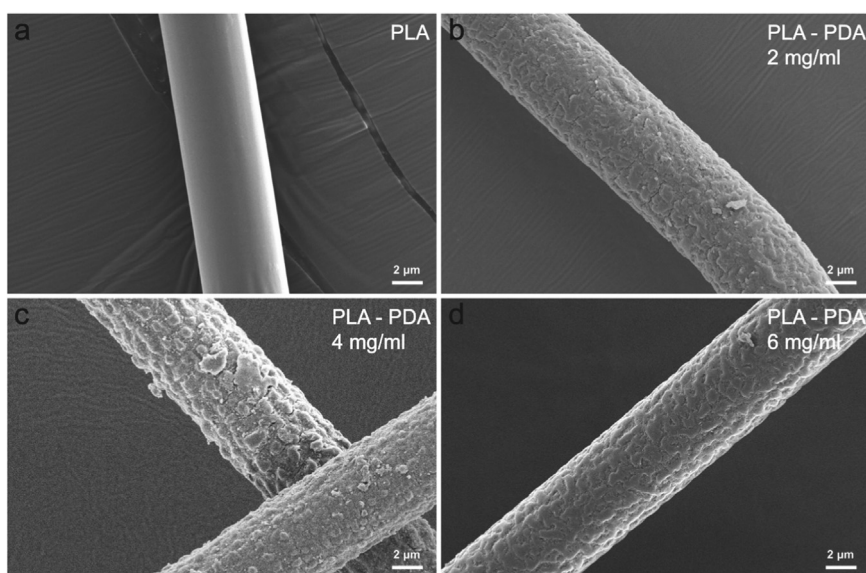


Fig. 5. SEM images of (a) PLA fibers and (b–d) PLA-PDA fibers formed at dopamine concentrations of 2, 4 and 6 mg/ml.

alendronate functionalization was observed. Based on these results, we selected a dopamine concentration of 6 mg/ml supplemented with EDA for further tests since this condition provided the highest amount of alendronate functionalization.

3.3. Fiber affinity for hydroxyapatite

Fig. S5 shows the affinity of pristine and modified PLA fibers for HA. At relatively short fiber length, alendronate-functionalized fibers seemed to adhere more abundantly to the surface of HA disks. These results confirm the specific affinity of bisphosphonates to bind to calcium, as observed previously by our group for alendronate-functionalized sub-micron PLLA fibers (Polini et al., 2017). However, alendronate-functionalized or alendronate-free PLA fibers adhered at comparable amounts for higher fiber lengths. These results can be explained by the gravitational forces which are more dominant for longer and/or thicker fibers.

3.4. Mechanical properties of CPCs reinforced with alendronate-functionalized PLA microfibers

Alendronate-functionalized PLA fibers were incorporated into CPC matrices and the resulting fiber-reinforced composites were subjected to flexural tests to study the effect of fiber amount, fiber length and alendronate modification on the flexural strength, modulus and work of fracture.

Fig. 7 presents the mechanical properties of CPCs reinforced with aminolyzed PLA fibers functionalized with alendronate using glutaraldehyde chemistry. The flexural strength of all samples varied within a relatively narrow range of 6.5–9 MPa; a significant increase in flexural strength relative to fiber-free CPC controls was only observed for cements containing 5 wt% of 3 mm long fibers (Fig. 7(a)), resulting into an almost 1.4-fold increase in the flexural strength of CPC-PLA-aminolyzed and CPC-PLA-ALE groups compared to unreinforced CPCs. The addition of aminolyzed or alendronate-functionalized PLA fibers to the CPC matrix did not alter the flexural modulus compared to the pure CPC. However, the fiber-free CPCs revealed WOF values between 50 and 60 J/m², whereas the addition of PLA fibers increased the toughness of the composites as evidenced by increased WOF values. Short fibers (1.2 mm and 1.7 mm) hardly toughened the CPCs (WOF < 200 J/m²), whereas the addition of long fibers of 3 mm resulted into a considerable increase in toughness (WOF between 750 and 1500 J/m²). Highest WOF values were observed for CPCs reinforced with 3 mm long PLA fibers at a 5 wt%. The functionalization of the microfibers with alendronate did not affect the toughness of CPCs compared to CPCs reinforced with PLA-aminolyzed fibers.

Fig. 8 presents the mechanical properties of CPCs reinforced with PDA-coated fibers or PDA-ALE modified fibers. In Fig. 8(a), the flexural strength values of fiber-free CPC reached ~ 6.5 MPa, whereas the addition of fibers generally increased the strength of the composite to values ranging from 8 to 11 MPa. A significant increase in flexural strength relative to fiber-free CPC controls was only observed for cements containing a high amount of fibers of 5 wt%, whereas fiber length (1.5 mm or 3 mm length) or the alendronate modification did not alter the flexural strength of the composite compared to fiber-free CPC. The flexural modulus of the composites was slightly affected by the fiber length or fiber weight fractions. The addition of pristine PLA fibers (2.5 wt%, 1.5 mm length) and alendronate-modified PLA fibers (2.5 wt%, 3 mm length) to the CPC matrix led to an increase in the flexural modulus compared to fiber-free CPC (Fig. 8(b)). In addition, CPC reinforced with alendronate-functionalized PLA fibers of 3 mm length (2.5 wt%) were stiffer than CPCs reinforced with unmodified PLA fibers. Generally, the flexural modulus of CPCs reinforced with PDA-modified fibers (Fig. 8(b)) was higher than the flexural modulus of CPCs reinforced with aminolyzed PLA fibers (Fig. 7(b)), even for fiber-free CPCs. These values were obtained using different mechanical

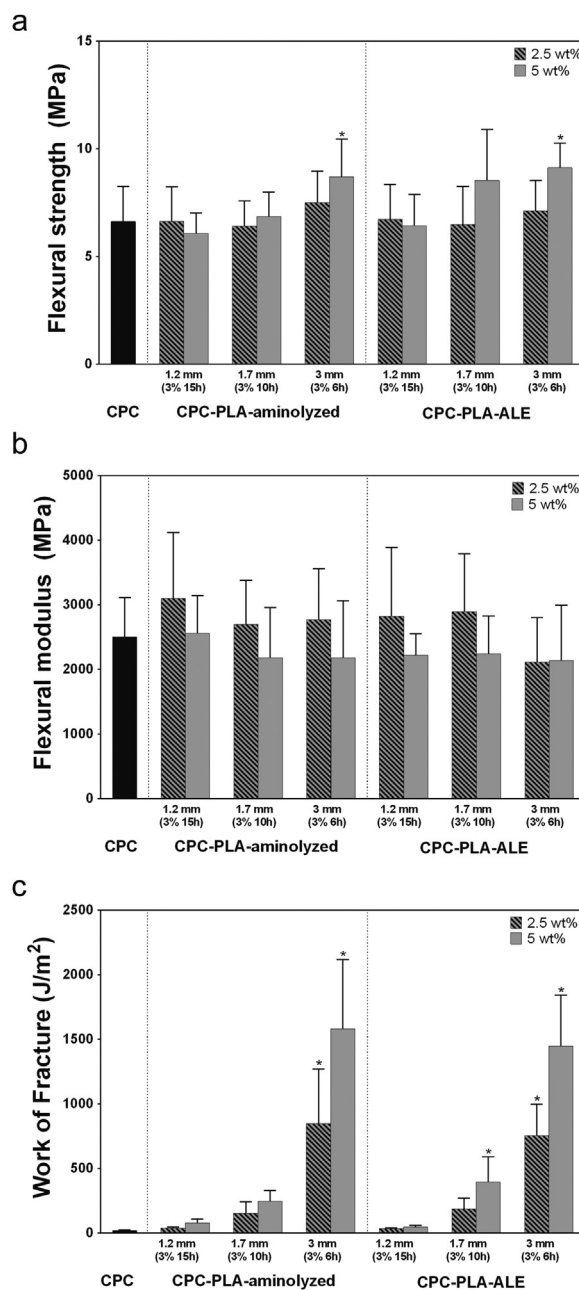


Fig. 7. Mechanical properties of fiber-free and fiber-reinforced CPCs containing aminolyzed PLA fibers conjugated with or without alendronate using glutaraldehyde chemistry: (a) flexural strength, (b) flexural modulus, (c) work of fracture; statistically significant differences vs. CPC controls are indicated with * ($p < 0.05$).

benches (see Section 2.5) which clearly affected the measurement of the flexural modulus values. However, measurements of flexural strength and toughness were not affected by the use of different benches. The toughness of CPCs increased almost 50-fold compared to fiber-free cements upon incorporation of PLA fibers into the cement. The toughness of the cements increased with increasing fiber length (3 vs. 1.5 mm) and amount (5 vs. 2.5 wt%), resulting into WOF values ranging from 750 to 1500 J/m². The functionalization of the PLA microfibers with alendronate did not affect the toughness of CPCs compared to CPCs reinforced with unmodified PLA or PLA-PDA fibers.

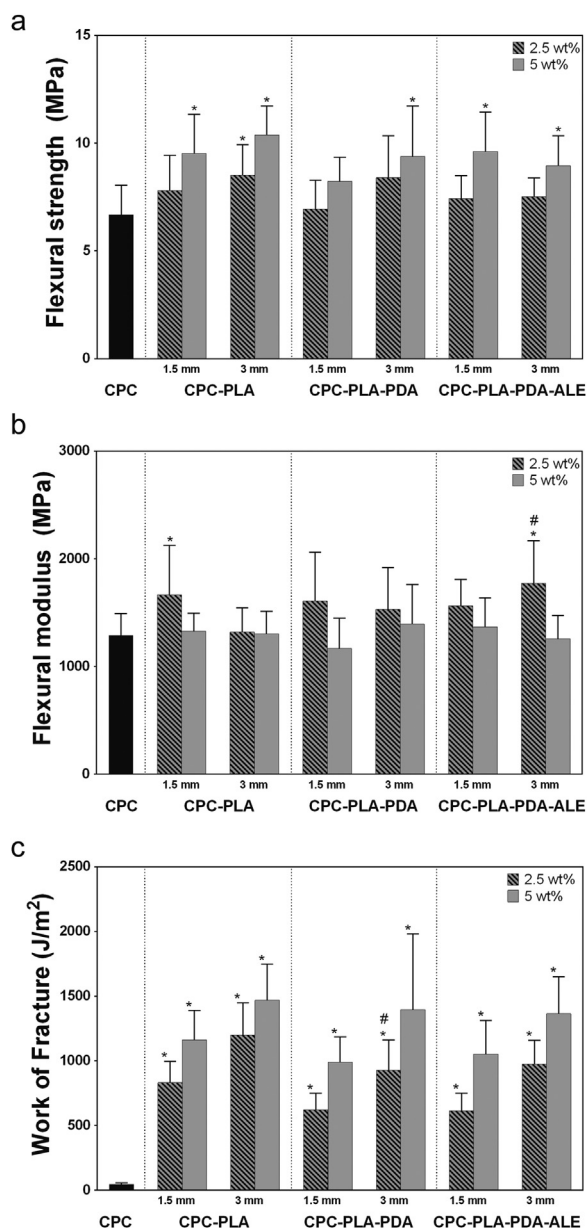


Fig. 8. Mechanical properties of fiber-free CPCs and fiber-reinforced CPCs containing PLA-PDA or PLA-PDA-ALE fibers: (a) flexural strength, (b) flexural modulus, (c) work of fracture; statistically significant differences are indicated with * (vs. CPC controls) and # (vs. CPC-PLA) ($p < 0.05$).

3.5. X-ray diffraction

X-ray diffractograms showed that all cements were converted to the apatite phase after 3 days of incubation in PBS (Fig. S6). No differences were observed when analyzing samples containing either 2.5 or 5% fiber weight fractions. This can be explained by the fact that a slightly altered powder-to-liquid ratio (from 0.5 to 0.52) did not alter the transformation of the crystal phases into calcium-deficient hydroxyapatite since the net quantity of CPC powder represented the majority of the composite material. Also, the different chemical functionalization methods did not alter the crystal phases of the cement composites.

3.6. Morphological assessment of fractured composite samples and nano-CT analysis

Fig. 9 presents the fracture surfaces of CPCs reinforced with aminolyzed PLA fibers functionalized or not with alendronate. For the CPCs reinforced with aminolyzed PLA fibers of 1.2 mm length, many fiber aggregates were observed that were in close contact with the cement matrix. At a higher magnification, we observed that a continuous interface was created between PLA-ALE fibers and the cement matrix, whereas space existed between PLA-aminolyzed fibers and the surrounding cement. For the CPCs reinforced with fibers of 1.7 mm length, clear signs of pull-out behavior were observed. These fibers could be discerned more clearly from the surrounding matrix as compared to the 1.2 mm long PLA fibers. The interface between the fibers and cement was similar for cements containing PLA-aminolyzed or PLA-ALE fibers. The cements reinforced with 3 mm long fibers, either aminolyzed or ALE functionalized, presented a similar morphology with the composites reinforced with 1.7 mm fibers (data not shown).

Fig. 10 presents the fracture surfaces of CPCs reinforced with manually cut unmodified PLA fibers, PLA-PDA fibers or PLA-PDA-ALE fibers of 1.5 mm length. For the CPCs reinforced with pristine PLA fibers, abundant pull-out behavior was observed characterized by empty circular holes. At the interface between these fibers and the surrounding cement a gap region was clearly observed. For CPCs reinforced with PLA-PDA and PLA-PDA-ALE fibers, pull-out behavior was less abundant. At a higher magnification, it was observed that cement remnants adhered to PLA-PDA fibers and PLA-PDA-ALE fibers without any substantial gap at the fiber-matrix interface. Unmodified PLA fibers, on the other hand, were not covered by cement remnants while the gap between functionalized fibers and cement matrix was larger. These results confirm that CaP particles adhered tightly to functionalized PLA fibers. For the composites reinforced with 3 mm long fibers, no additional morphological differences were observed (data not shown).

Finally, nano-CT analysis was performed on the fractured specimens after flexural testing to investigate the dispersion of PLA-ALE (movies SV1 and SV2) and PLA-PDA-ALE fibers (movies SV3 and SV4) within the cement matrix in 3D. At a 2.5% fiber weight, the fibers were more homogeneously distributed when compared to the 5 wt% for both groups, whereas the dispersion was predominantly heterogeneous at a fiber amount of 5 wt%, as indicated by areas of agglomerated fibers. However, for the PLA-PDA-ALE composite samples, the extent of fiber agglomeration was lower. Moreover, we used nano-CT to quantify the fiber volume within the composites as shown in Fig. S7. These results revealed that the actual fiber volume increased from ~ 3 to $\sim 7\%$ v/v for cements containing 2.5 vs. 5 wt% of PLA-ALE fibers, respectively.

4. Discussion

The efficacy of fiber reinforcement of ceramic matrices depends strongly on the fiber-matrix adhesion, but this crucial parameter is hardly addressed so far in literature on fiber-reinforcement of bio-ceramic matrices. Biodegradable fibers made of polyesters such as PLA have been widely used to toughen calcium phosphate cements, but the affinity of these hydrophobic polymers to hydrophilic cement matrices is typically poor. Therefore, we functionalized PLA fibers with alendronate groups that possess a strong affinity for the Ca^{2+} ions present in calcium phosphate cements.

In this study, three different strategies were employed to conjugate alendronate onto the surface of PLA fibers and enhance their affinity to the cement matrix. We first exploited a wet-chemical aminolysis procedure to tune the length of discrete PLA fibers and introduce amine functionalities for further covalent attachment of alendronate using either glutaraldehyde or Michael addition chemistry. Michael addition reactions are known for their selectivity and for the stability of the generated bonds, which can be considered as an advantage compared to

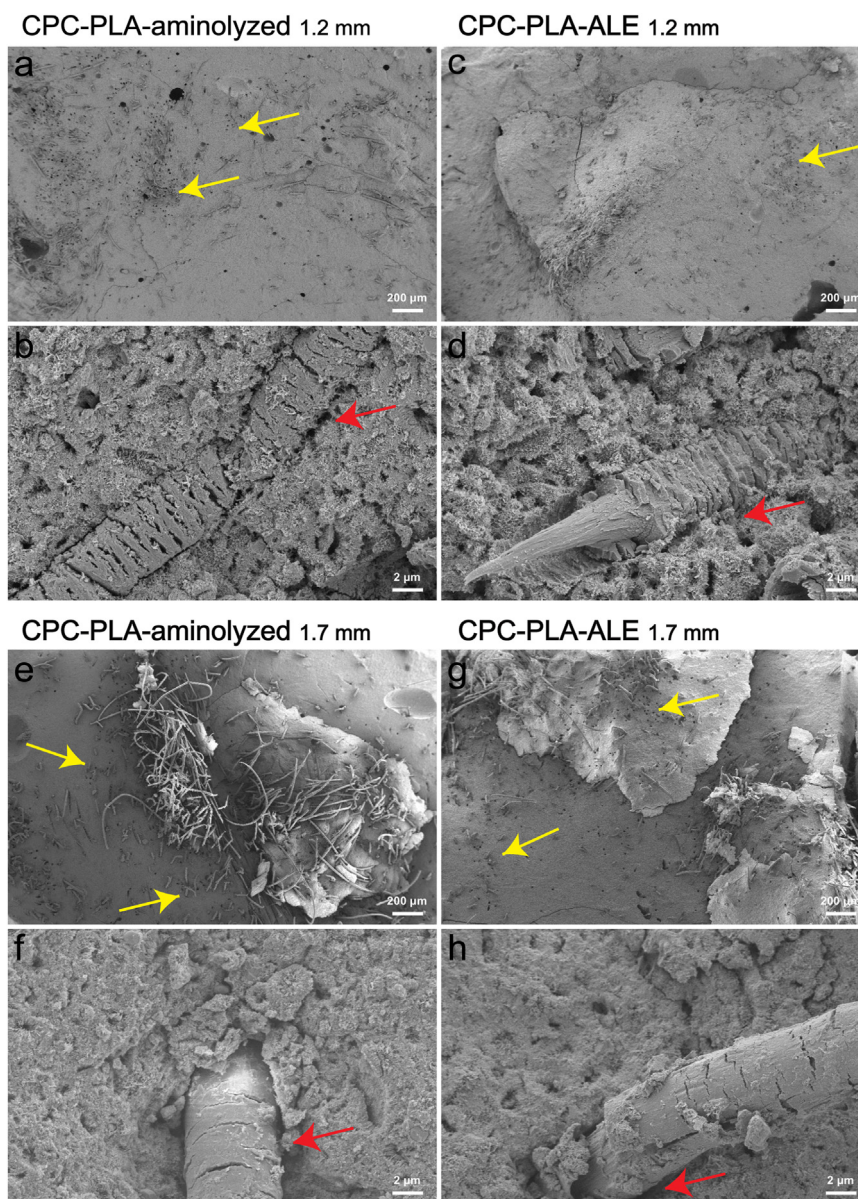


Fig. 9. Fracture surfaces of fiber-reinforced CPCs after three-point flexural testing: (a–b) CPC with 2.5 wt% PLA-aminolyzed fibers and (c–d) PLA-ALE functionalized fibers of 1.2 mm length, (e–f) CPC with 2.5 wt% PLA-aminolyzed fibers and (g–h) PLA-ALE functionalized fibers of 1.7 mm length; yellow and red arrows indicate pull-out behavior and fiber-matrix interface, respectively.

the lability of imine bonds formed through glutaraldehyde chemistry (Navarro et al., 2017). Nevertheless, our results showed that the amount of conjugated alendronate on the surface of PLA fibers was similar for both types of conjugation chemistries (Fig. 4), which suggests that the surface of PLA fibers was saturated with an equal amount of alendronate groups for both types of conjugation reactions. In view of the more complex and time-consuming Michael addition reaction, glutaraldehyde chemistry was selected as a functionalization strategy for further experiments. To decouple fiber cutting from alendronate conjugation, we also developed an aminolysis-independent functionalization strategy by means of manual cutting of the fibers and subsequent polydopamine immobilization followed by conjugation of alendronate onto the fibers through glutaraldehyde chemistry. Polydopamine immobilization layers have been extensively investigated during the past decade due to their remarkable capability to adhere to any type of substrate and provide secondary reactivity for further chemical functionalization with a wide variety of groups (Kang et al., 2012; Lee et al., 2007, 2009). By using this aminolysis-independent

method, we were able to increase the amount of amine groups and consequently the alendronate conjugation to $\sim 20 \mu\text{g ALE/mg}$ of fibers, which was a 3-fold increase as compared to the amount of alendronate conjugation onto aminolyzed PLA fibers ($\sim 6.5 \mu\text{g ALE/mg}$ of fibers). We successfully enhanced the reactivity of polydopamine layers for alendronate by the addition of amines to the dopamine precursor solution, thereby enriching the polydopamine layer with functional amine groups to improve the efficacy of subsequent chemical modifications further (Yang et al., 2014, 2015). Using this method, we obtained a maximum plateau value of $\sim 35 \mu\text{g ALE/mg}$ of fibers, whereas the amount of alendronate conjugation was only $20 \mu\text{g ALE/mg}$ of fiber for the ethylenediamine-free polydopamine immobilization method. These results are in agreement with previous studies, which confirmed that both covalent and non-covalent interactions were formed upon the addition of amines to polydopamine layers (Yang et al., 2015). Thus, we showed that the addition of ethylenediamine to dopamine precursor solutions is an effective strategy to enhance the chemical reactivity of polydopamine layers. The formation of these polymeric intermediate

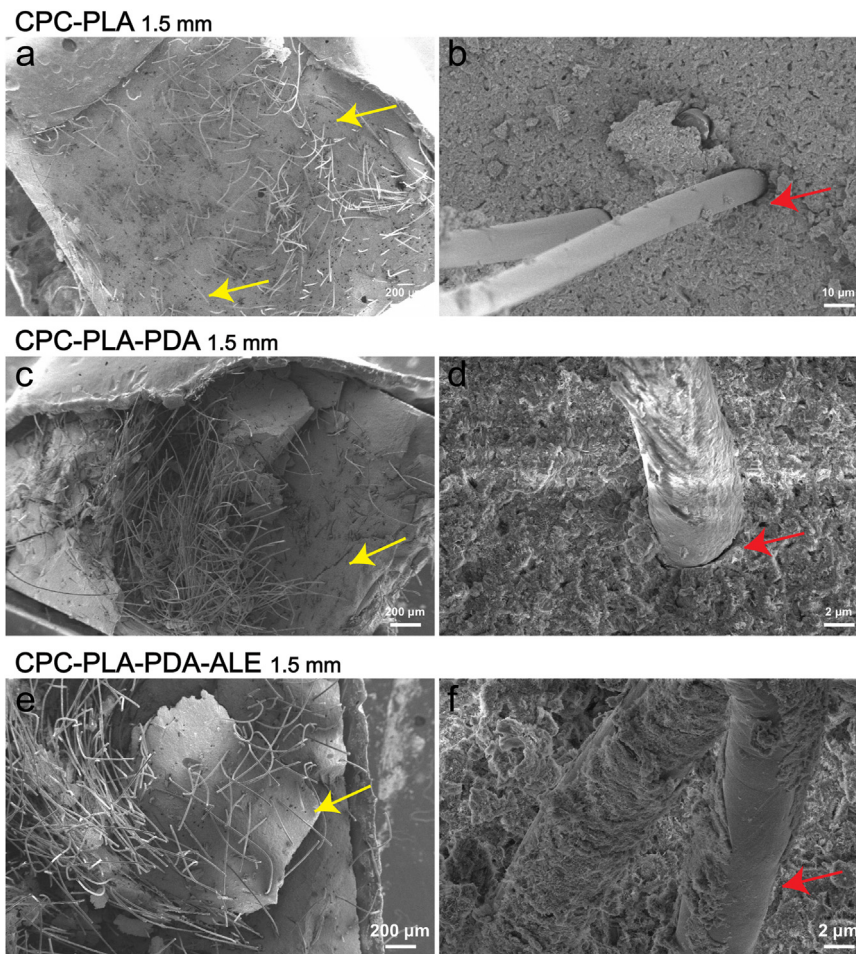


Fig. 10. Fracture surfaces of fiber-reinforced CPCs after three-point flexural testing: (a–b) CPC with 2.5 wt% PLA fibers of 1.5 mm length, (c–d) CPC with 2.5 wt% PLA-PDA fibers of 1.5 mm length; (e–f) CPC with 2.5 wt% PLA-PDA-ALE functionalized fibers of 1.5 mm length; yellow and red arrows indicate pull-out behavior and fiber-matrix interface, respectively.

layers was confirmed by using scanning electron microscopy (Fig. 5) corroborated with FTIR analysis (Fig. S3), which revealed the formation of polydopamine layers with submicron roughness. Obviously, these intermediate layers were much thicker than the single layers formed upon conjugation of alendronate onto aminolyzed PLA fibers, which explains the higher amounts of alendronate conjugation using the polydopamine-assisted immobilization strategy.

Both manually and chemically cut PLA fibers functionalized with alendronate using glutaraldehyde chemistry were selected for further studies on their reinforcing efficacy upon incorporation into calcium phosphate cements. As shown in Fig. 7(a), the incorporation of PLA-aminolyzed fibers hardly increased the flexural strength of fiber-free CPC, whereas the addition of manually cut PLA fibers resulted into an increase of the flexural strength of up to 11 MPa. As demonstrated in previous studies (Zhang and Xu, 2005), fiber strength and stiffness strongly determine the efficacy of fiber reinforcement. The lack of a strengthening effect caused by aminolyzed fibers can be explained by the deteriorating effect of the aminolysis procedure on the integrity of the PLA fibers, which is evident from the electron micrographs in Figs. 9(b) and 9(d). Generally, the flexural strength and modulus of the CPCs was hardly affected by the alendronate modification of both manually and chemically cut PLA fibers.

Generally, all CPCs reinforced with manually cut PLA fibers were toughened considerably, but aminolyzed fibers only enhanced the toughness of CPC at the highest fiber length of 3 mm (both for 2.5 and 5 wt% of fibers). These results confirmed again the damaging effect of the aminolysis procedure on PLA fibers, thus stressing the crucial

importance of the mechanical integrity of fibers for reinforcement of CPCs. Regarding the manually cut PLA fibers, we observed that the toughness of CPCs reinforced with 1.5 mm long PLA fibers (WOF values between 600 and 1200 J/m²) was about 2–3 times higher than samples reinforced with aminolyzed PLA fibers with a comparable length of 1.7 mm (~ 400 J/m²). On the other hand, the toughness of CPCs reinforced with either aminolyzed or manually cut fibers of 3 mm length was comparable, confirming that the shortest aminolysis time corresponding to this fiber length did not compromise the mechanical integrity of the PLA fibers. Finally, the functionalization of manually cut fibers with alendronate did not improve the toughness of CPCs as compared to samples reinforced with unmodified PLA fibers, even though alendronate modification of PLA fibers increases their affinity for hydroxyapatite (Polini et al., 2017). An alternative approach to improve the adhesion of PLA fibers to CPCs was based on the treatment of PLA fibers with an oxygen plasma treatment, which improved fiber wettability and the toughness of fiber-reinforced CPCs (Canal et al., 2014) up to WOF values of 400 kJ/m². However, these values are still far from clinical needs since the WOF of cortical adult bone ranges between 1.5 and 15 kJ/m² (Currey and Butler, 1975). In this study, we managed to obtain WOF values of up to 1.5 kJ/m² which are close to the lowest values reported for cortical bone.

From the SEM images presented in Fig. 9, we observed a gap between PLA-ALE fibers of 1.7 mm length, while PLA-ALE fibers of 1.2 mm showed a continuous interface between the fiber surface and cement matrix. This result could be explained by the increased amount of PLA-ALE functionalized on 1.2 mm fibers (6.5 μg ALE/mg of fiber) vs.

1.7 mm fibers (2.5 μg ALE/mg of fiber), which allowed for a stronger adhesion to the cement particles. In Fig. 10, it was shown that hydroxyapatite crystals adhered to the PLA-PDA fibers, which was not observed for smooth, unmodified PLA fibers. In addition, pull-out behavior of pristine PLA fibers was also more abundant compared to chemically functionalized PLA fibers. Finally, we observed that the interface between the PLA-PDA fibers and cement was more compact and tightly connected as compared to the gap observed between unmodified PLA fibers and the surrounding matrix. This further confirms that PLA fibers adhered more tightly to calcium phosphate crystals upon modification with polydopamine or alendronate. These results are in line with a previous study which reported that catecholamine moieties not participating in substrate adhesion can bind to Ca^{2+} ions in hydroxyapatite (Ryu et al., 2010). However, it should be emphasized that fiber alignment might have also affected the formation of gaps between fibers and the CPC matrix. Generally, fibers aligned transversally to the tensile stresses causing specimen fracture did not reveal gaps between the fiber surface and the cement, indicating that the affinity between the CPC matrix and fiber surface was sufficiently strong to prevent detachment of fibers from the surrounding matrix (e.g. Fig. 10(e)). Fibers aligned longitudinally to the direction of tensile stresses occasionally revealed gaps between the fibers and the matrix (e.g. Fig. 10(b) and 10(d)), which might be caused by an irreversible reduction in fiber diameter due to plastic deformation upon tensile loading prior to fiber pullout.

Generally, however, this study did not reveal a significant improvement of cement toughness resulting from alendronate modification of PLA fibers. Based on the results from us as well as other groups we assume that toughening of CPCs using PLA fibers is mainly limited by the mechanical properties of the PLA fibers rather than the affinity of these fibers for the cement matrix. In addition, we observed in the nano-CT reconstruction movies (supplementary videos SV1–SV4) that all types of fibers agglomerated in CPCs. This heterogeneous distribution of the fibers inside the CPC might have been caused by the manual mixing procedure. Hence, poor fiber dispersion within the matrix was another factor which compromised the efficacy of fiber reinforcement using PLA fibers.

Supplementary material related to this article can be found online at [doi:10.1016/j.jmbbm.2018.11.003](https://doi.org/10.1016/j.jmbbm.2018.11.003).

In addition, we speculate that the accessibility of the alendronate groups conjugated to the surface of PLA fibers was suboptimal. Previous studies showed that conjugation of alendronate onto poly(D,L-lactide-co-glycolide) (PLGA) nanoparticles using polyethylene glycol (PEG) spacers allowed for tuning of the affinity between PLGA nanoparticles and HA (Choi and Kim, 2007). Herein, alendronate groups were directly coupled onto the surface of both chemically and manually cut PLA fibers, which might have limited their mobility and thus reactivity towards HA. The formation of intermediate PDA layers obviously allowed for immobilization of higher amounts of alendronate distanced further away from the smooth PLA substrate. Nevertheless, the mobility of these alendronate groups might also have been limited by the high molecular weight of dense polydopamine layers. As shown previously, after only 40 min of polydopamine deposition, the effective molecular weight of these polydopamine layers was reaching millions of Da (Lee et al., 2007). Although the surface roughness of polydopamine-functionalized PLA fibers was considerably increased upon polydopamine immobilization, the roughness of the formed PDA layers did not enhance the strength and stiffness properties of the resulting cement composites. Apparently, frictional sliding between these fibers and the cement matrix was not affected by fiber roughness. However, the improved toughness of the composites reveals that there is sufficient physical or chemical interaction between functionalized PLA fibers and the surrounding ceramic matrix.

5. Conclusion

The present study investigated if the efficacy of fiber reinforcement of calcium phosphate cements (CPCs) could be improved by conjugating calcium-binding alendronate groups onto the surface of polylactic acid (PLA) fibers. Alendronate was successfully conjugated onto the surface of chemically or manually cut PLA fibers using three different conjugation strategies. The amount of alendronate conjugation could be tuned by controlled aminolysis of PLA fibers or by the deposition of an amine-enriched intermediate polydopamine layer. Reinforcement of CPCs with manually cut PLA fibers resulted into a significantly improved toughness as compared to the reinforcement using fibers chemically cut by controlled aminolysis since the aminolysis procedure compromised the mechanical integrity of the PLA fibers. Functionalization of PLA fibers with alendronate did not significantly improve the strength or elastic modulus of the resulting composites. However, the improved toughness of the composites reveals that there is sufficient physical or chemical interaction between functionalized PLA fibers and the surrounding ceramic matrix to reinforce the cements through different mechanisms.

Acknowledgements

This work was supported by the Dutch Technology Foundation (NWO, VIDI grant #13455). The authors declare that they do not have any conflict of interest.

Appendix A. Supplementary material

Supplementary data associated with this article can be found in the online version at [doi:10.1016/j.jmbbm.2018.11.003](https://doi.org/10.1016/j.jmbbm.2018.11.003).

References

- Bohner, M., 2001. Physical and chemical aspects of calcium phosphates used in spinal surgery. *EurSpine J.* 10 (Suppl. 2), S114–S121. <https://doi.org/10.1007/s005860100276>.
- Canal, C., Gallinetti, S., Ginebra, M.P., 2014. Low-pressure plasma treatment of polylactide fibers for enhanced mechanical performance of fiber-reinforced calcium phosphate cements. *Plasma Process Polym.* 11 (7), 694–703. <https://doi.org/10.1002/ppap.201400018>.
- Castro, A.G.B., Polini, A., Azami, Z., Leeuwenburgh, S.C.G., Jansen, J.A., Yang, F., van den Beucken, J., 2017. Incorporation of PLLA micro-fillers for mechanical reinforcement of calcium-phosphate cement. *J. Mech. Behav. Biomed. Mater.* 71, 286–294. <https://doi.org/10.1016/j.jmbbm.2017.03.027>.
- Causa, F., Battista, E., Della Moglie, R., Guarnieri, D., Iannone, M., Netti, P.A., 2010. Surface investigation on biomimetic materials to control cell adhesion: the case of RGD conjugation on PCL. *Langmuir* 26 (12), 9875–9884. <https://doi.org/10.1021/la100207q>.
- Choi, S.W., Kim, J.H., 2007. Design of surface-modified poly(D,L-lactide-co-glycolide) nanoparticles for targeted drug delivery to bone. *J. Control Release* 122 (1), 24–30. <https://doi.org/10.1016/j.jconrel.2007.06.003>.
- Currey, J.D., Butler, G., 1975. The mechanical properties of bone tissue in children. *J. Bone Jt. Surg. Am. Vol.* 57 (6), 810–814.
- Gunnella, F., Kunisch, E., Bungartz, M., Maenz, S., Horbert, V., Xin, L., Mika, J., Borowski, J., Bischoff, S., Schubert, H., Hortschansky, P., Sachse, A., Illerhaus, B., Gunster, J., Bossert, J., Jandt, K.D., Ploger, F., Kinne, R.W., Brinkmann, O., 2017. Low-dose BMP-2 is sufficient to enhance the bone formation induced by an injectable, PLGA fiber-reinforced, brushite-forming cement in a sheep defect model of lumbar osteopenia. *Spine J.* 17 (11), 1699–1711. <https://doi.org/10.1016/j.spinee.2017.06.005>.
- Kang, S.M., Hwang, N.S., Yeom, J., Park, S.Y., Messersmith, P.B., Choi, I.S., Langer, R., Anderson, D.G., Lee, H., 2012. One-step multipurpose surface functionalization by adhesive catecholamine. *Adv. Funct. Mater.* 22 (14), 2949–2955. <https://doi.org/10.1002/adfm.201200177>.
- Kim, T.G., Park, T.G., 2008. Biodegradable polymer nanocylinders fabricated by transverse fragmentation of electrospun nanofibers through aminolysis. *Macromol. Rapid Commun.* 29 (14), 1231–1236. <https://doi.org/10.1002/marc.200800094>.
- Kruger, R., Groll, J., 2012. Fiber reinforced calcium phosphate cements – on the way to degradable load bearing bone substitutes? *Biomaterials* 33 (25), 5887–5900. <https://doi.org/10.1016/j.biomaterials.2012.04.053>.
- Larsson, S., Hannink, G., 2011. Injectable bone-graft substitutes: current products, their characteristics and indications, and new developments. *Injury* 42 (Suppl. 2), S30–S34. <https://doi.org/10.1016/j.injury.2011.06.013>.
- Lee, H., Dellatore, S.M., Miller, W.M., Messersmith, P.B., 2007. Mussel-inspired surface chemistry for multifunctional coatings. *Science* 318 (5849), 426–430. <https://doi.org/10.1126/science.1141728>.

- [org/10.1126/science.1147241](https://doi.org/10.1126/science.1147241).
- Lee, H., Rho, J., Messersmith, P.B., 2009. Facile conjugation of biomolecules onto surfaces via Mussel adhesive protein inspired coatings. *Adv. Mater.* 21 (4), 431–434. <https://doi.org/10.1002/adma.200801222>.
- Li, G., Yang, P., Liao, Y., Huang, N., 2011. Tailoring of the titanium surface by immobilization of heparin/fibronectin complexes for improving blood compatibility and endothelialization: an in vitro study. *Biomacromolecules* 12 (4), 1155–1168. <https://doi.org/10.1021/bm101468v>.
- Maenz, S., Brinkmann, O., Kunisch, E., Horbert, V., Gunnella, F., Bischoff, S., Schubert, H., Sachse, A., Xin, L., Gunster, J., Illerhaus, B., Jandt, K.D., Bossert, J., Kinne, R.W., Bungartz, M., 2017. Enhanced bone formation in sheep vertebral bodies after minimally invasive treatment with a novel, PLGA fiber-reinforced brushite cement. *Spine J.* 17 (5), 709–719. <https://doi.org/10.1016/j.spinee.2016.11.006>.
- Maenz, S., Hennig, M., Muhlstadt, M., Kunisch, E., Bungartz, M., Brinkmann, O., Bossert, J., Kinne, R.W., Jandt, K.D., 2016. Effects of oxygen plasma treatment on interfacial shear strength and post-peak residual strength of a PLGA fiber-reinforced brushite cement. *J. Mech. Behav. Biomed. Mater.* 57, 347–358. <https://doi.org/10.1016/j.jmbbm.2016.01.030>.
- Maenz, S., Kunisch, E., Muhlstadt, M., Bohm, A., Kopsch, V., Bossert, J., Kinne, R.W., Jandt, K.D., 2014. Enhanced mechanical properties of a novel, injectable, fiber-reinforced brushite cement. *J. Mech. Behav. Biomed. Mater.* 39, 328–338. <https://doi.org/10.1016/j.jmbbm.2014.07.028>.
- Navarro, R., Monrde, C., Molina, S., Perez-Perrino, M., Reviriego, F., del Prado, A., Gallardo, A., Reinecke, H., 2017. Understanding the regioselectivity of Michael addition reactions to asymmetric divinyl compounds. *Rsc Adv.* 7 (89), 56157–56165. <https://doi.org/10.1039/c7ra11005g>.
- Pascaud, P., Errassifi, F., Brouillet, F., Sarda, S., Barroug, A., Legrouri, A., Rey, C., 2014. Adsorption on apatitic calcium phosphates for drug delivery: interaction with bisphosphonate molecules. *J. Mater. Sci. Mater. Med.* 25 (10), 2373–2381. <https://doi.org/10.1007/s10856-014-5218-0>.
- Polini, A., Petre, D.G., Iafisco, M., de Lacerda Schickert, S., Tampieri, A., van den Beucken, J., Leeuwenburgh, S.C.G., 2017. Polyester fibers can be rendered calcium phosphate-binding by surface functionalization with bisphosphonate groups. *J. Biomed. Mater. Res. A* 105 (8), 2335–2342. <https://doi.org/10.1002/jbm.a.36077>.
- Polini, A., Wang, J., Bai, H., Zhu, Y., Tomsia, A.P., Mao, C., 2014. Stable biofunctionalization of hydroxyapatite (HA) surfaces by HA-binding/osteogenic modular peptides for inducing osteogenic differentiation of mesenchymal stem cells. *Biomater. Sci.* 2, 1779–1786. <https://doi.org/10.1039/C4BM00164H>.
- Ryu, J., Ku, S.H., Lee, H., Park, C.B., 2010. Mussel-inspired polydopamine coating as a universal route to hydroxyapatite crystallization. *Adv. Funct. Mater.* 20 (13), 2132–2139. <https://doi.org/10.1002/adfm.200902347>.
- Uquillas Paredes, J.A., Polini, A., Chrzanoski, W., 2014. Protein-based biointerfaces to control stem cell differentiation. In: Huttmacher, D., Chrzanoski, W. (Eds.), *Biointerfaces*. The Royal Society of Chemistry, Cambridge, pp. 3–29.
- Varghese, O.P., Sun, W., Hilborn, J., Ossipov, D.A., 2009. In situ cross-linkable high molecular weight hyaluronan-bisphosphonate conjugate for localized delivery and cell-specific targeting: a hydrogel linked prodrug approach. *J. Am. Chem. Soc.* 131 (25), 8781–8783. <https://doi.org/10.1021/ja902857b>.
- Wang, H., Boerman, O.C., Sariibrahimoglu, K., Li, Y., Jansen, J.A., Leeuwenburgh, S.C., 2012. Comparison of micro- vs. nanostructured colloidal gelatin gels for sustained delivery of osteogenic proteins: bone morphogenetic protein-2 and alkaline phosphatase. *Biomaterials* 33 (33), 8695–8703. <https://doi.org/10.1016/j.biomaterials.2012.08.024>.
- Xu, H.H., Quinn, J.B., 2002. Calcium phosphate cement containing resorbable fibers for short-term reinforcement and macroporosity. *Biomaterials* 23 (1), 193–202. [https://doi.org/10.1016/S0142-9612\(01\)00095-3](https://doi.org/10.1016/S0142-9612(01)00095-3).
- Yang, Y., Qi, P., Wen, F., Li, X., Xia, Q., Maitz, M.F., Yang, Z., Shen, R., Tu, Q., Huang, N., 2014. Mussel-inspired one-step adherent coating rich in amine groups for covalent immobilization of heparin: hemocompatibility, growth behaviors of vascular cells, and tissue response. *ACS Appl. Mater. Interfaces* 6 (16), 14608–14620. <https://doi.org/10.1021/am503925r>.
- Yang, Y., Qi, P.K., Ding, Y.H., Maitz, M.F., Yang, Z.L., Tu, Q.F., Xiong, K.Q., Leng, Y., Huang, N., 2015. A biocompatible and functional adhesive amine-rich coating based on dopamine polymerization. *J. Mater. Chem. B* 3 (1), 72–81. <https://doi.org/10.1039/c4tb01236d>.
- Zhang, Y., Xu, H.H., 2005. Effects of synergistic reinforcement and absorbable fiber strength on hydroxyapatite bone cement. *J. Biomed. Mater. Res. A* 75 (4), 832–840. <https://doi.org/10.1002/jbm.a.30461>.
- Zuo, Y., Yang, F., Wolke, J.G., Li, Y., Jansen, J.A., 2010. Incorporation of biodegradable electrospun fibers into calcium phosphate cement for bone regeneration. *Acta Biomater.* 6 (4), 1238–1247. <https://doi.org/10.1016/j.actbio.2009.10.036>.